Laser-Induced Conversion of Noble Metal-Island Films to Dense Monolayers of Spherical Nanoparticles

Mitsuo Kawasaki* and Mitsuhiro Hori

Department of Molecular Engineering, Graduate School of Engineering, Kyoto University, Yoshida, Kyoto 606-8501, Japan

Received: March 26, 2003

By postdeposition nanosecond laser irradiation at 532 nm with a relatively low laser fluence of typically ~50 mJ/cm^2, Ag- and Au-island films sputter-deposited on mica could be converted to a dense monolayer of spherical nanoparticles 40−60 nm in average diameter without aggregation. The peak position and good sharpness of the corresponding surface plasmon (SP) resonance suggested no significant interparticle SP interactions for the dense two-dimensional arrays of spherical nanoparticles tens of nanometers in diameter. In higher laser fluence regime above 100 mJ/cm^2 or more, a complicated mode of film conversion resulting in strong deformation (flattening) of the SP band became dominant before the ablation mode finally set in. A crude estimate of the instantaneous temperature of the metal-island films as a function of laser fluence suggested that laser-induced melting is probably the major driving force for the conversion to good spherical nanoparticle films.

Introduction

The optical properties of metal nanoparticles have long been of interest in physical chemistry from both theoretical and practical viewpoints,[1] and are still the subjects providing various new research opportunities in connection to the growing attention to nanoscale materials technology and engineering. Among others, Ag and Au nanoparticles are known for their strong surface plasmon (SP) resonance in the visible region, which is also believed to play a crucial role for the well-known surface-enhanced Raman spectroscopy (SERS).[2] Their characteristic extinction spectra depend on many factors such as the particle size, shape, degree of interparticle interactions, dielectric environment, and so forth,[1] and the recent studies concerning highly nonspherical particles such as nanorods[3,4] and nanoprisms[5,6] demonstrate how remarkably one can modify the optical properties by sophisticated shape control.

Recently, there has been also considerable interest in the laser-induced shape changes of noble metal nanoparticles,[4,7−16] which not only provide a simple means for "post-preparation" shape control but also pertain to the physically important issue of laser−nanoparticle interactions and some complicated relaxation dynamics of the deposited laser energy.[12] Among others, the laser-induced transformation of Au nanorods in colloidal solution to spherical particles represents a particularly drastic shape change, and has been studied in detail by Link and coworkers using both femtosecond and nanosecond laser pulses.[11−13] They pointed out an important role of heat transfer to the surrounding solvent (on the 100 ps time scale) as the major factor that accounts for the large difference between femtosecond and nanosecond lasers in the threshold laser fluence and in the detailed structural dynamics involved. The laser-induced shape change was also reported for Ag nanoparticles embedded in glass matrixes,[14−16] and the results, as compared to those in colloidal solution, are indicative of some significant impact of the rigid glass matrix.

In this article, we newly illuminate the effect of nanosecond laser irradiation (at 532 nm) to Ag- and Au-island films sputter-deposited on a mica substrate. Such metal-island films often consist of oblate spheroidal particles not completely separated from each other (i.e., more often coalesced than not),[17,18] and known to serve as good SERS active substrates.[18] Together with some wide distribution in the particle size and shape, this morphology generally yields much broader and red-shifted SP resonance as compared to that expected for isolated spherical particles. One of the merits of this system is in that virtually all the nanoparticles in the metal-island film, even though significantly coagulated, are in the equivalent condition with respect to the incoming laser flux, so one needs just a single laser pulse to study the whole aspect of laser−nanoparticle interactions. Besides, each particle is in contact with the solid substrate on one side but otherwise exposed (in the present work) to the ambient air. This not only considerably changes the dynamics of dissipation of deposited laser energy as compared to that in solution or in glass, but also allows the vaporization mode (at high laser fluence) to be clearly distinguished from melting and other modes, simply because the evaporated atoms are irreversibly lost into the environment. Correlation between these phase behaviors and the input laser energy will thus yield useful additional information for better understanding the fundamental physics of laser-induced nanoparticle shape change.

Another important motivation of this work is the expectation that by laser irradiation with appropriate energy density, the metal-island film may be converted to a dense monolayer of nanoparticles or colloidal film with far better defined particle shape without aggregation. This could be indeed verified in the present work. The feasibility of direct analysis of the particle shape and distribution by atomic force microscopy (AFM) imaging is another noteworthy advantage of this system. Unlike many other conventional methods for preparation of Ag and Au nanoparticles, the thus-prepared colloidal film is free from

* Corresponding Author: Tel (Fax): (+81)-75-753-5540. E-mail: Kawasaki@ap6.kuic.kyoto-u.ac.jp.

10.1021/jp034768s CCC: $25.00
Published on Web 06/24/2003

any protective material, and if required, can be chemically modified or derivatized by many different kinds of molecular species at a later time. Such a dense colloidal film with and without its surface chemical modification may be useful as a simple model system for exploring some unique optical or spectroscopic properties potentially caused by the interaction or coupling of SP with molecular excitations[2,19] in addition to the well-known SERS. The extinction spectra of dense 2D arrays of nanoparticles are also useful to experimentally address the question[20−24] of how closely the metal particles need to be spaced for the interparticle SP interactions to become really significant.

Experimental Section

Both Ag and Au island films were grown on freshly cleaved natural mica by a simple DC glow discharge sputtering method in a pure Ar atmosphere. This simple method was originally introduced by this group for preparation of atomically flat, high-quality Au(111) and Ag(111) films.[25,26] The deposition time was typically around 5 min in our standard deposition conditions that yield ∼4 nm/min deposition rate. The deposition temperature was set at ∼200 °C for Ag and ∼300 °C for Au, respectively. The choice of deposition temperature is not very crucial for preparation of metal-island films, but the employed conditions ensured the formation of films with least broad SP bands for metal-island films.

The laser-irradiation experiment was carried out in the ambient atmosphere by using the second harmonic of an Nd: Yag laser (Continuum, Minilite-10) at 532 nm. The available laser power was 13 mJ/pulse with the pulse width of ∼5 ns. The incident beam size at the film surface (placed vertically with respect to the light path) was adjusted by focusing or defocusing the original laser beam through a convex lens, so that the laser fluence at the film surface could be changed for about 2 orders of magnitude from ∼10 mJ/cm^2 up to ∼3 J/cm^2.

The extinction spectra of the sample film were measured in the transmission mode by using a multichannel analyzer (Hamamatsu Photonics Co., PMA-11) as the photodetector. For samples irradiated with laser beam sizes less than 1 mm (high laser fluence), the center of the laser-irradiated small spot was probed in combination with an optical Nikon microscope with a halogen lamp as the light source. The shortest wavelength examined in this case was limited to 400 nm. In the case of other samples for which the irradiated spot size was greater than 2 mm in diameter, the shorter limit of wavelength in the measured spectra could be extended to 300 nm (the sensitivity limit of PMA-11) in an optical setup without the microscope and with a Xe lamp as an alternative light source.

AFM images were taken for a limited number of typical sample films at Toray Research Center, Inc. on our request. The microscope was a NanoScope IIIa (Digital Instruments) operated in the tapping mode. The probe was an Si cantilever (Olympus Optical Co., Ltd., OMCL-AC160TS-W2) scanned typically at ∼0.2 Hz along the *X*-direction. The images were obtained within 2 days after sample preparation, because the laser-processed samples slowly underwent a noticeable change in color when kept in the ambient atmosphere for several days.

Results

Ag-Island Film. Figure 1 shows typical extinction spectra measured for the Ag-island films before (broken lines) and after (solid lines) a single laser shot at relatively low laser fluence of ∼50 mJ/cm^2. The two sets of spectra represent two different levels of effective mass thickness expected to fall in the 15−30 nm range. It can be seen that the broad SP bands associated with the as-deposited island films were transformed by the laser irradiation to markedly sharp (∼60 nm in fwhm) and blue-shifted (peaked at 430 nm) bands. It is quite remarkable for a monolayer film of Ag nanoparticles (see below) to give the peak optical density up to ∼0.9 while preserving such a sharp band shape. The main peak at 430 nm most likely arises from dipole SP resonance of spherical Ag nanoparticles in the given dielectric environment, and the clearly visible subpeak at ∼350 nm, attributed to quadrapole SP resonance,[1] is indicative of the presence of relatively large Ag particles near ∼50 nm or more in diameter. It should be also noted that we found very little further change in the extinction spectra by multiple (up to 100) laser shots in the given fluence condition around 50 mJ/cm^2/pulse.

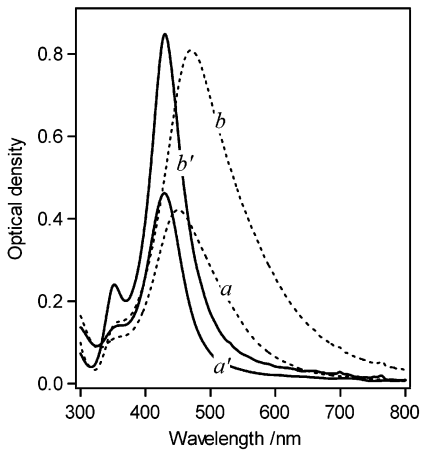

Figure 1. Typical extinction spectra of Ag-island films for two different levels of effective mass thickness, taken before (*a*, *b*; broken lines) and after (*a*′, *b*′; solid lines) single laser pulse irradiation at ∼50 mJ/cm^2.

Successful conversion to a dense monolayer of spherical Ag nanoparticles by laser irradiation is further evidenced by the couple of typical AFM images shown in Figure 2. Here, we have chosen films with relatively small effective mass thickness (corresponding to spectra *a* and *a*′ in Figure 1) to gain better resolution of particle shape, but the observed packing density was already quite large. The image of as-deposited Ag-island film (Figure 2a) may give the impression that the film appears to consist of rather small, separate Ag nanoparticles densely packed side by side. Care should be taken, however, in interpreting such AFM images (contour mapped), because even continuous metal films with finely rugged surface morphology would produce an analogous image as if they consisted of separate particles. In fact, as shown below the image of Figure 2a, a typical cross-sectional height profile along a line connecting the centers of neighboring bright spots can be simulated by a series of oblate particles significantly overlapped (or coagulated) with each other.

After the laser irradiation, the AFM image (Figure 2b) increased its image contrast considerably and exhibited more circular (apparently larger) bright spots, in accordance with the shape transition to spherical particles causing greater up−down movement of the AFM cantilever as it passes over each particle. A typical cross-sectional profile given below the image can indeed be simulated by a series of spherical particles that are very closely spaced or touching each other. The particle size distribution in this image is shown by the histogram on the right, which suggests that the distribution is roughly Gaussian with an average diameter of ∼40 nm. The effective coverage of these nanoparticles in terms of their total projective area relative to

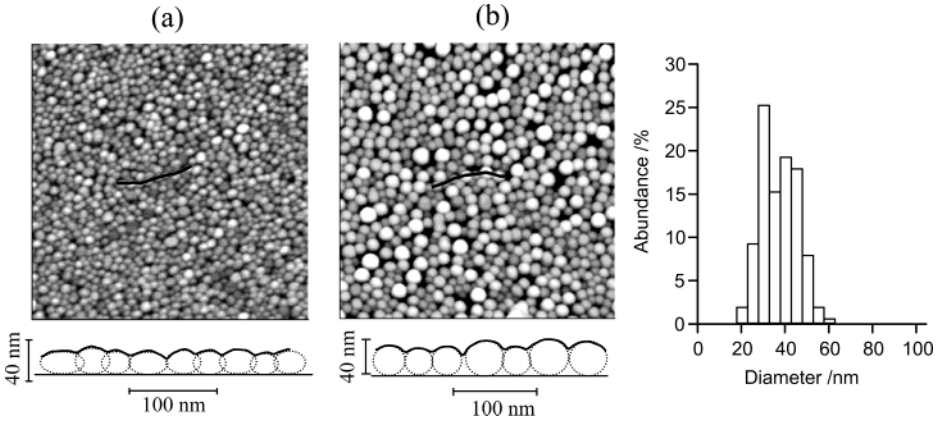

Figure 2. (a) 1000 × 1000 nm^2 AFM image of as-deposited Ag-island film taken for sample producing a peak optical density of 0.4−0.5 in its broad SP band (corresponding to spectrum *a* in Figure 1). Shown below the image is a height profile along the line (drawn in the middle region of the image) connecting through the centers of neighboring bright spots, together with a series of model oblate spheroids simulating the measured height profile. (b) 1000 × 1000 nm^2 AFM image taken after laser irradiation (single shot at ∼50 mJ/cm^2). A typical height profile given below the image can be simulated by a dense array of spherical Ag nanoparticles, with size distribution as shown on the right.

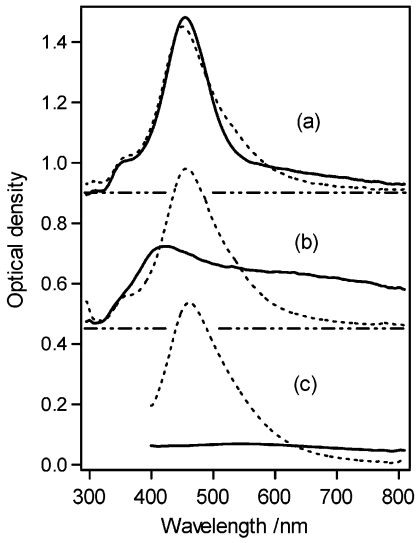

Figure 3. A series of extinction spectra showing the effect of laser irradiation in the conditions of laser fluence in short [(a)] or in excess [(b) and (c)] of energy for the conversion to spherical Ag nanoparticles. Broken-line spectra are for the as-deposited Ag-island films for reference, and solid-line spectra for samples after single laser pulse irradiation at selected laser fluence of (a) ∼30 mJ/cm^2, (b) ∼300 mJ/cm^2, and (c) ∼3 J/cm^2, respectively. Spectra in (a) and (b) are vertically offset to avoid overlaps; two horizontal lines indicate corresponding baselines.

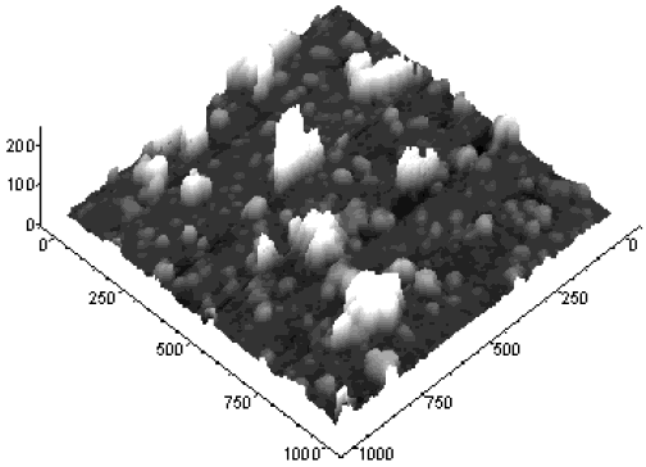

Figure 4. 1000 × 1000 nm^2 gray-scaled 3D image of Ag-island film taken after high fluence (∼300 mJ/cm^2) laser irradiation, uncovering a rough film morphology responsible for the flattening of the SP band (cf. Figure 3b).

that of the substrate was estimated to be as large as ∼70%, not very far from that (90.7%) for the closest (hexagonal) 2D packing of spheres. Despite this remarkably high packing density, there is no implication of any serious aggregation. Note that there is no protective material present in this system. Furthermore, the fact that the SP band remains so sharp (as seen in Figure 1) at this high packing density suggests that, in 2D arrays of spherical nanoparticles tens of nm in diameter, substantial overlap or coalescence of nearby particles is necessary for interparticle SP interactions to become really significant.

As expected, it was only in some limited range of laser fluence, from ∼40 to ∼90 mJ/cm^2, that the above mode of film conversion to spherical nanoparticles was dominant. Below this range, e.g., at ∼30 mJ/cm^2, the observed change in the extinction spectra was just a partial bleaching of the SP band around the laser wavelength (532 nm) as exemplified in Figure 3a, and no spectral change could be noticed at fluence below ∼20 mJ/cm^2. The selective partial bleaching of the SP band in the region of laser wavelength represents a laser-induced depletion of particles with SP resonance in that region, and was observed also in the work using a colloidal solution of Au nanorods.[11,12] By contrast, the behaviors in the high laser fluence regime seemed quite unique to the island film on solid substrate. Namely, at e.g., ∼300 mJ/cm^2, the original SP band was strongly flattened at a substantial optical density level (see Figure 3b), suggesting that the film was converted to something that did not necessarily retain the nature of normal Ag nanoparticles. Increasing the laser fluence further up to ∼3 J/cm^2 then nearly eliminated the extinction in the whole spectral region (Figure 3c), indicating that laser ablation or vaporization finally set in.

We found that the strong deformation of the SP band (Figure 3b) observed before the onset of the ablation mode was associated with such a rough surface morphology as imaged in Figure 4, which gives us the impression that the island film as a whole suffered considerable damage by the laser beam rather than a simple shape change of Ag nanoparticles. Another important fact is that the film in this state exhibited much stronger adhesion to the mica substrate as compared to the as-deposited island films and the spherical nanoparticle films, which were both easily wiped off the mica substrate. We therefore interpret that the laser irradiation at this high fluence caused a large amount of heat to be transferred from the "hot" Ag-islands to a thin surface layer of the underlying mica

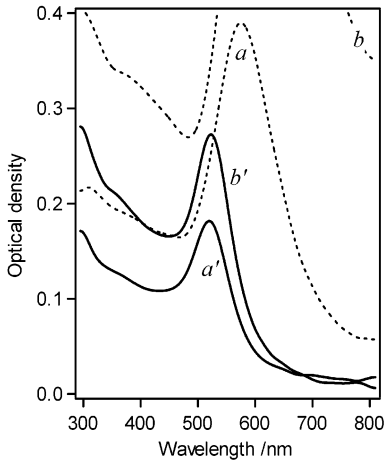

Figure 5. Typical extinction spectra of Au-island films taken before (*a* and *b*) and after (*a*′ and *b*′) single laser pulse irradiation at ~50 mJ/cm^2.

substrate, thereby causing its surface roughening together with some elemental mixing between Ag and mica. This most naturally accounts for the increased film adhesion to mica and also for the distinct flattening of the SP band. It should be also noted that this process involving significant heat loss to the mica substrate could actually begin at much lower laser fluence of, for example, ~80 mJ/cm^2 or less, though to a far smaller extent so that it became noticeable only by multiple laser irradiations. There, a single laser shot still resulted predominantly in the conversion to spherical nanoparticles as mentioned above, but upon repeated laser irradiations (typically at 10 Hz) the extinction spectra were gradually broadened again and eventually (after more than 50 pulses) flattened out to produce a spectrum similar to that shown in Figure 3b.

Au-Island Films. The interaction between the nanosecond laser and Au-island films caused quite analogous changes in the film morphology and nanoparticle shape depending on the laser fluence, though there were of course some important differences in finer aspects. As shown in Figure 5, the laser-induced (again at relatively low laser fluence of ~50 mJ/cm^2) spectral change was apparently more drastic in this case, causing large reduction in optical density as a whole. The remaining spectra exhibited a sharp SP resonance at 520 nm with a band shape very close to that usually observed for spherical colloidal solution. This large reduction in optical density by laser irradiation must still reflect primarily a laser-induced shape change, and does not represent any substantial loss of Au mass that would not be possible in the given fluence condition of ~50 mJ/cm^2 (see the discussion below). In addition, according to the relationship between the light extinction efficiency of a metal nanosphere and its complex bulk dielectric constant,[1] the comparatively small peak optical density below 0.3 after the laser irradiation is just what one can expect for a dense-enough monolayer of spherical Au nanoparticles.

The above interpretations are further supported by the AFM images presented in Figure 6, which uncovers a dramatic laser-induced change in the film morphology and nanoparticle shape. As evident both from the image contrast and from the typical cross-sectional profile given below the image, the original island film (Figure 6a) consists of markedly flat-shaped particles. Since the film, by extended deposition, grows to an atomically flat Au(111) film, the flattened particle surfaces most probably represents (111) facets. It must be this specific film morphology (together with some substantial overlap of nearby particles) that is responsible for the intense, broad SP bands of the original Au-island films noted above (Figure 5).

After the laser irradiation, Au nanoparticles more perfectly spherical than in the case of Ag emerged (Figure 6b) with wider size distribution (see the histogram given on the right) and with appreciably lower packing density. Some of them exceed even 100 nm in diameter, and it seems that some nearby particles in the original island film could merge into a single sphere. Together with the large shape change from slab-like to spherical particles, this accounts for a wider interparticle spacing than in the case of Ag. Note, however, that the specific coverage of these spheres in Figure 6b is still as high as ~50%, even though the film imaged here represents a relatively small effective mass thickness that gives the peak optical density smaller than 0.2 (spectrum *a*′ in Figure 5).

As for the effect of laser fluence, it was qualitatively very similar to that noted for the Ag-island films; excess laser fluence likewise causing strong flattening of the SP band accompanied by large increase in the film adhesion to mica, and finally laser ablation of the majority of Au islands. One noteworthy difference is in that successful conversion to spherical Au nanoparticles by single laser shot was allowed in an apparently wider range of laser fluence up to ~150 mJ/cm^2.

Discussion

As mentioned in the Introduction and confirmed by the experimental results, nanosecond laser irradiation of Ag- and Au-island films resulted in several distinguishable modes of film conversion, depending on the laser fluence. Thus, by analyzing

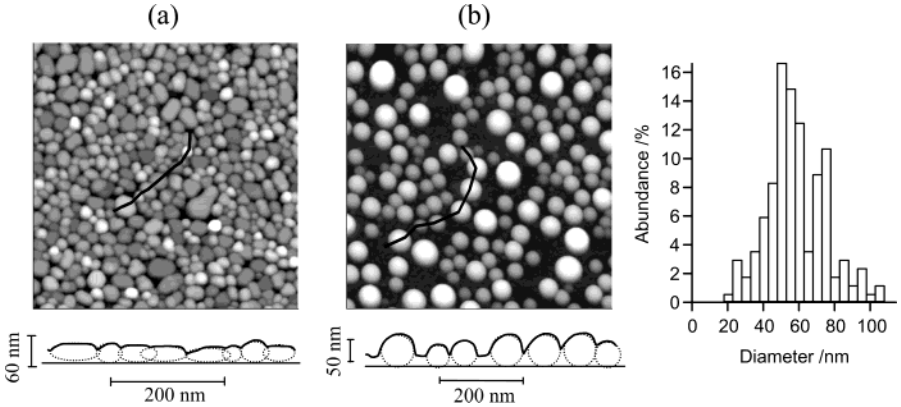

Figure 6. (a) 1000 × 1000 nm^2 AFM image of as-deposited Au-island film (corresponding to that producing spectrum *a* in Figure 5) consisting of flat-shaped particles as simulated below the image. (b) 1000 × 1000 nm^2 AFM image taken after laser irradiation (single shot at ~50 mJ/cm^2), clearly evidencing conversion to good spherical nanoparticles, with a typical height profile and size distribution shown below the image and on the right, respectively.

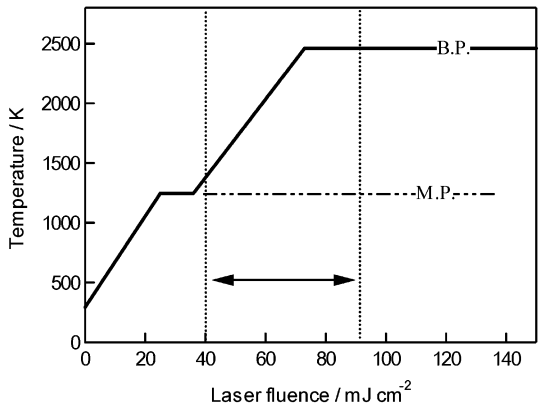

Figure 7. Estimated temperature of Ag-island film with effective film thickness of ~20 nm as a function of laser fluence. An intermediate narrow plateau shows the region where temperature is maintained at the melting point (mp) and the next wide plateau corresponds to the boiling point (bp). The arrow between two vertical lines indicates the range of laser fluence where a single laser shot led to conversion to spherical Ag nanoparticle films.

their relationships carefully, we may gain better insight into the nature of the laser−nanoparticle interactions and their thermal consequences. To do so, it would be useful to estimate the instantaneous temperature that an island film can reach in the ~5 ns laser period as a function of laser fluence. A similar temperature estimate was made also in the previous works on laser-induced shape changes in colloidal solution[10,12] by using the bulk thermal parameters of Ag and Au (specific heat capacity and heat of melting and vaporization).

We first estimate from our standard film deposition rate together with the topographic information from the AFM images that a typical effective mass thickness of Ag- and Au-island films used in this work was ~20 nm. The most difficult part of the temperature estimate here is concerned with the question of how much heat was transferred to the substrate and to the air environment on what time scale. As mentioned above, our results in fact suggested a large heat loss to the mica substrate, which is presumably fast enough to compete with energy uptake during the laser pulse period of ~5 ns.[12] Below, we tentatively and rather arbitrarily assume that roughly half of the laser energy absorbed by the island film is effectively used for its temperature rise and phase transition, if any. For the typical film thickness assumed above, the fraction of the incident laser energy at 532 nm absorbed by the island films is estimated to be ~40% from the extinction spectra. We assume this to be constant for the entire pulse period (~5 ns), although this gives some serious overestimate at high laser fluence, where the shape change and/or vaporization (resulting in a large reduction in effective light absorptance at 532 nm) may proceed on the time scale much shorter than the laser pulse width.

The calculated temperature (T) is plotted as a function of laser fluence in Figure 7 for the Ag-island film. Our calculation did not cover the region where T can formally exceed the boiling point. There, the whole metal should be in the gas phase, thus having no relevance for the experimental results. Although Figure 7 is based on many assumptions and approximations mentioned above, it provides a fair rationale for our experimental observations within the framework of the thermal model. Namely, Figure 7 suggests that the laser fluence below 20 mJ/cm^2, where only slight or no laser-induced changes were observed, is insufficient to cause even partial melting of the Ag islands. More importantly, the experimental range of laser fluence (indicated by two vertical lines and arrow), where successful conversion to good spherical nanoparticles was observed, approximately fits in the region where T is expected to lie between the melting and boiling points. The fit may become even better if we take into account the aforementioned fact that the absorbed laser energy tends to be overestimated more at higher laser fluence. This means that the upper limit of fluence that keeps T between the melting and boiling points can be higher than Figure 7 suggests. In any case, the conversion to good spherical nanoparticles can be understood easily on the basis of the surface free energy consideration for fully liquidized Ag particles.

The result of a similar temperature estimate for the Au-island film also correlated reasonably with the experimental results. The thermal parameters for a 20 nm thick Au film and its effective light absorption at 532 nm result in quite a similar temperature rise profile as a function of laser fluence to that shown in Figure 7. Then, the similar melting points of Ag and Au (1234 K vs 1336 K) but significantly higher boiling point of Au (3129 K) than that of Ag (2435 K) expand the range of laser fluence that yields temperatures between the melting and boiling points. This is at least in qualitative agreement with the fact that conversion to good spherical nanoparticles was allowed in a wider range of laser fluence for Au-island films.

The spherical nanoparticles formed in this way had relatively large sizes distributed well over 50 nm in diameter. Thus this mode of film conversion does not compare to the laser-induced size reduction or fragmentation previously reported for colloidal solution.[7−10] In the framework of the thermal model, such modes of shape change involving substantial loss or partition of the particle mass would not be possible at temperatures below the boiling point. In practice, a similar process may be possible also in the present system at increased laser fluence, but it would be masked by the two alternative high fluence modes, particularly by the one involving a thermal damage of the mica substrate and causing strong deformation of the SP band. Note in addition that this mode could set in at laser fluence much lower than that needed to cause a massive vaporization of the metal islands (ablation mode), and thus could still preserve most of the mass initially deposited on the substrate.

It seems that both the average size and the size distribution of the spherical nanoparticles formed by the laser irradiation somehow mirror those of the more-or-less coagulated particles in the original island film. This conversely implies that we might be able to gain better size control for the dense spherical nanoparticle films by more sophisticated control over the morphology of the initial island film. What seems also worth investigating in the same context is the effect of in-site laser irradiation in the middle of the island film formation that will probably give strong influence on the nucleation and growth of the metal-island films.

Summary and Conclusions

In summary, we observed that Ag- and Au-island films sputter-deposited on mica could be converted to a dense monolayer or 2D array of spherical nanoparticles without aggregation by postdeposition nanosecond laser irradiation at 532 nm in a relatively narrow range of laser fluence. The resultant film gave strongest possible SP bands for a monolayer of spherical nanoparticles without any serious broadening. These nanoparticles are essentially free from any protective material, and may be easily modified and derivatized by many different kinds of molecular species if necessary at a later time.

In the high laser fluence regime, the conversion to spherical nanoparticles was taken over by two other distinguishable modes, one causing strong flattening of the SP band and likely

involving a heat damage of the mica substrate and some elemental mixing between the metal and mica. At laser fluence more excess in energy, the ablation mode finally set in.

A crude estimate of the temperature of the metal-island films as a function of laser fluence gave support for the thermal model of laser-induced shape change, suggesting that laser-induced melting is probably the major driving force for the conversion of the Ag- and Au-island films to good spherical nanoparticle films.

References and Notes

(1) Kelly, K. L.; Coronado, E.; Zhao, L. L.; Schatz, G. C. *J. Phys. Chem. B* **2003**, *107*, 668.

(2) See, for example, Franzen, S.; Folmer, C. W.; Glomm, W. R.; O'neal, R. *J. Phys. Chem. B* **2002**, *106*, 6533, and references therein.

(3) Yu, Y.-Y.; Chang, S.-S.; Lee, C.-L.; Wang, C. R. C. *J. Phys. Chem. B* **1997**, *101*, 6661.

(4) Chang, S.-S.; Shih, C.-W.; Chen, C.-D.; Lai, W.-C.; Wang. C. R. C. *Langmuir* **1999**, *15*, 701.

(5) Jin, R.; Cao, Y.-W.; Mirkin, C. A.; Kelly, K. L.; Schatz, G. C.; Zheng, J. G. *Science* **2001**, *294*, 1901.

(6) Mock, J. J.; Barbic, M.; Smith, D. R.; Schultz, D. A.; Schultz, S. *J. Chem. Phys.* **2002**, *116*, 6755.

(7) Takami, A.; Yamada, H.; Nakano, K.; Koda, S. *Jpn. J. Appl. Phys.* **1996**, *35*, L781.

(8) Kamat, P. V.; Flumiani, M.; Hartland, G. V. *J. Phys. Chem. B* **1998**, *102*, 3123.

(9) Kurita, H.; Takami, A.; Koda, S. *Appl. Phys. Lett.* **1998**, *72*, 789.

(10) Takami, A.; Kurita, H.; Koda, S. *J. Phys. Chem. B* **1999**, *103*, 1226.

(11) Link, S.; Burda, C.; Mohamed, M. B.; Nikoobakht, B.; El-Sayed, M. A. *J. Phys. Chem. A* **1999**, *103*, 1165.

(12) Link, S.; Burda, C.; Nikoobakht, B.; El-Sayed, M. A. *J. Phys. Chem. B* **2000**, *104*, 6152.

(13) Link, S.; Wang, Z. L.; El-Sayed, M. A. *J. Phys. Chem. B* **2000**, *104*, 7867.

(14) Stepanov, A. L.; Hole, D. E.; Bukharaev, A. A.; Townsend, P. D.; Nurgazizov, N. I. *Appl. Surf. Sci.* **1998**, *136*, 298.

(15) Kaempfe, M.; Rainer, T.; Berg, K. J.; Seifert, G.; Graener, H. *Appl. Phys. Lett.* **1999**, *74*, 1200.

(16) Kaempfe, M.; Hofmeister, H.; Hopfe, S.; Seifert, G.; Graener, H. *J. Phys. Chem. B* **2000**, *104*, 11847.

(17) Royer, P.; Goudonnet, J. P.; Warmack, R. J.; Ferrell, T. L. *Phys. Rev. B* **1987**, *35*, 3753.

(18) Van Duyne, R. P.; Hulteen, J. C.; Treichel, D. A. *J. Chem. Phys.* **1993**, *99*, 2101.

(19) Sato, T.; Tsugawa, F.; Tomita, T.; Kawasaki, M. *Chem. Lett.* **2001**, 402.

(20) Laor, U.; Schatz, G. C. *Chem. Phys. Lett.* **1981**, *82*, 566.

(21) Laor, U.; Schatz, G. C. *J. Chem. Phys.* **1982**, *76*, 2888.

(22) Yang, W.-H.; Schatz, G. G.; Van Dyune, R. P. *J. Chem. Phys.* **1995**, *103*, 869.

(23) Lazarides, A. A.; Schatz, G. C. *J. Chem. Phys.* **2000**, *112*, 2987.

(24) Lazarides, A. A.; Schatz, G. C. *J. Phys. Chem. B* **2000**, *104*, 460.

(25) Kawasaki, M.; Uchiki, H. *Surf. Sci.* **1997**, *388*, L1121.

(26) Kawasaki, M. *Appl. Surf. Sci.* **1998**, *135*, 115.